Preparation of a Composite of Polyacrylate and Nano-SiO_2 Particles and Evaluation of its Performance of Oil-Water Mixture Treatment

Yanjia Zhou,[a] Feng Li,[a,b] Guihong Lan,[a*] Yongqiang Liu,[c] Haiyan Qiu,[a] Bo Xu,[a] Keyu Pu,[a] Wenren Dai,[a] Xinyang Zhang,[a]

a. Southwest Petroleum University, Department of Chemistry and Chemical Engineering, Chengdu, 610500, China.

b. Yibin Tianyuan Group Co., Ltd., Yibin 644004, China.

c. Faculty of Engineering and Physical Sciences, University of Southampton, Southampton, UK.

[*]Corresponding author: Guihong Lan

Tel: +86 18980710384, Email: guihonglan416@sina.com

Abstract

To acquire a material with simultaneous oil-water emulsion demulsification and oil-absorbing performance, SiO_2 nanoparticles were introduced into the acrylate polymerization system to prepare oil absorbent SiO_2/P (SMA-*co*-MMA-*co*-BA) (PSA-SiO_2). PSA-SiO_2 was synthesized from monomers and functional materials, including methyl methacrylate (MMA), butyl acrylate (BA), octadecyl methacrylate (SMA) and SiO_2 hydrophobically modified by vinyltrimethoxysilane (VTMS). The molecular structure of PSA-SiO_2 was characterized by FT-IR, and its morphology was observed using SEM. In addition, the optimal synthesis conditions for the polymerization system, such as the monomer ratio, the amount of crosslinker and stabilizer and then the particle size and dose of SiO_2, were discussed in detail. PSA-SiO_2 had a decent oil absorbency for pure halogenated and aromatic hydrocarbons (49.10, 56.41, 47.32, 43.45, 36.22, and 30.14 g/g for CH_2Cl_2, $CHCl_3$, CCl_4, C_2Cl_4, toluene and styrene, respectively). Furthermore, SiO_2, as a functional material, makes composites that possess excellent demulsification properties for oil-in-water emulsions. The oil removal efficiency of $CHCl_3$ in Tween 80-stabilized and CTAB-stabilized emulsions were 94.88% and 98.11%, respectively. All results indicated that PSA-SiO_2 had valuable potential for oil removal and emulsion treatment.

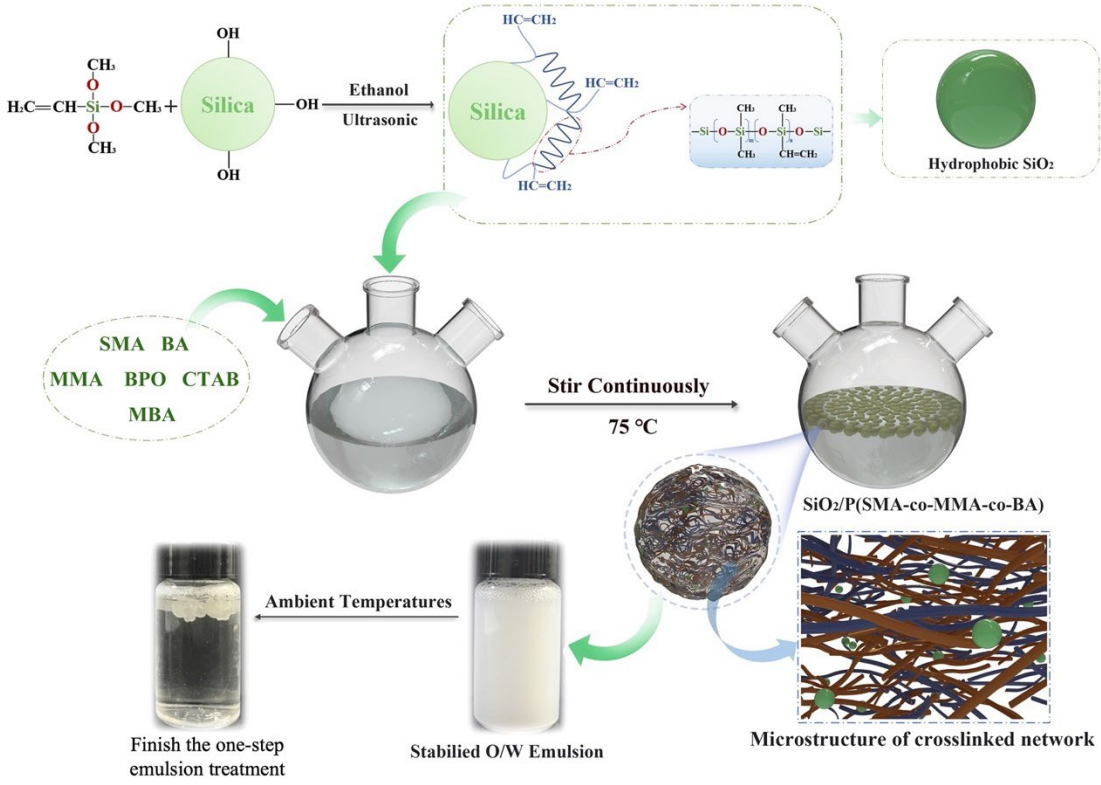

Graphical abstracts

Highlights

● An organic-inorganic composite was synthesized by suspension polymerization

● The composite was applied for absorbing pure oil or removing oil form water

● By modification, the composite acquired the demulsification ability

● The composite accomplished one-step demulsification and emulsion treatment

● The oil absorption and emulsion treatment could achieve at room temperature

Key word: Composite materials; Chemical synthesis; Demulsification.

1. Introduction

Halogenated and aromatic hydrocarbons are typical nonaqueous phase liquids (NAPLs). They enter the water environment through the unreasonable emission of industrial wastewater and domestic sewage and improper leakage of toxic chemical wastes[1]. These NAPLs, including chloroform, toluene, styrene, etc., easily accumulate in water bodies and can even cause bioaccumulation, which is harmful to the environment and mutagenic, carcinogenic and teratogenic to human cells[2,3]. Therefore, the removal of certain common NAPLs from water is a pressing issue in oily

wastewater treatment.

Normally, oil-absorbing materials are used to grab oil in water and separate the oil-water miscible phase quickly and efficiently[4,5]. According to in-depth research on oil-absorbing materials in recent decades, synthetic polymers with porous and three-dimensional network structures have several advantages over other traditional oil absorbents, such as excellent oil retention, rapid adsorption, environmentally friendly materials, strong oil absorbency and easy recovery[6]. Zhang et al.[7] synthesized a porous alumina microsphere/acrylic ester resin (AER) hybrid by suspension polymerization and showed that the oil absorbency for $CHCl_3$ and CCl_4 reached 29.85 and 27.00 g/g, respectively. Yan et al. [8] successfully prepared an acrylate oil-absorbing resin by suspension polymerization with biomorphic hollow MgO fibers as inorganic components. The results suggested that the oil absorbencies of the resin to $CHCl_3$, CCl_4 and toluene were 28.22, 25.23 and 15.13 g/g, respectively. In addition, the resin still had good oil absorbency and reusability after six adsorption-desorption recycling processes. Liu et al. [9] prepared spherical magnetic oil-absorbing resins (MPOARs) by introducing photosensitive functional compounds and magnetic particles into the polymerization system. And the oil absorbencies to CH_2Cl_2, $CHCl_3$, and toluene were 19.7, 18.4 and 11.7 g/g, respectively. Additionally, the resin satisfied the requirement of effortless recovery under magnetic conditions.

The oil absorbents in the aforementioned studies had a strong oil absorbency to partially common halogenated and aromatic hydrocarbons and developed more distinctive properties by introducing functional materials. However, these materials exhibited oil-absorbing performance and were only used for stratified oil-water mixtures. It was difficult to remove oil from emulsified oil-water mixtures. The NAPLs accumulated in water bodies form stable water-in-oil (W/O) and oil-in-water (O/W) emulsions following the migration process, and the emulsions treatment is more challenging than layered oil removal from water[10].

Nisar Ali et al.[11] designed a raspberry-like magnetic composite demulsifier with strong interfacial activity. This material not only showed favorable interfacial activity at the oil-water interface but could also break crude oil-water emulsions entirely within one hour at 60 °C. In addition, the demulsifier recovered without complications due to its timely response to the external magnetic field. You mu et al.[12] synthesized a concave nanoparticle demulsifier that had satisfactory interfacial activity and amphiphilicity. The demulsification efficiency of this material was as

high as 96.7% at neutral pH and atmospheric temperature.

The demulsifiers mentioned in the above studies had excellent demulsification competence, but the oil after demulsification still remained in the aqueous environment and required additional processing. In addition, most demulsifiers are amphiphilic at the oil-water interface because of the great stability of emulsions and interfacial activity, so their service conditions are harsh routinely[13, 14]. Therefore, it is essential to develop materials that integrate demulsification and oil absorption to achieve an uncomplicated one-step treatment of oil-water emulsions.

The polyacrylate materials were superhydrophobic and could swell in oils. So, they had good adsorption capacity to a range of commonly used halogenated hydrocarbons and aromatic hydrocarbons, but they were invalid at degrading oil-water emulsions[15]. In addition, acrylic ester compounds could be polymerized with various modified materials to obtain specific functional properties. For example, introducing basalt fiber (BF) to acrylic ester polymerization systems reinforced the tensile and flexural strengths of the modified polymer[16], while adding functional monomers such as acrylated epoxidized linseed oil (AELO) or acrylated epoxidized methyl ester (AEMA) improved adhesion strength and enhanced tackiness of the modified polymer[17,18].

Thus, in this study, we introduced modified silica with tri-block in the polyacrylate system. It was expected to destabilize the oil-water interface and thus achieve demulsification. Moreover, SiO_2, as a porous inorganic nanoparticle, had the potential to enrich the multihole structure of polymers and enlarge the contact area between oil and oil absorbent. Thus, we synthesized the SiO_2/P (SMA-*co*-MMA-*co*-BA) composite (PSA-SiO_2) by introducing the modified inorganic nanoparticle SiO_2 as a functional material to prepare an oil absorbent with octadecyl methacrylate (SMA), methyl methacrylate (MMA) and butyl acrylate (BA) as monomers. The performance of emulsion treatment of PSA-SiO_2 was evaluated in detail, and then the mechanism of the one-step process of emulsion treatment was discussed. The prepared composite could accomplish one-step demulsification and absorption of demulsified oil at room temperature. Our work is expected to bring new ideas to the development of materials for oily wastewater treatment.

2. Materials and methods

2.1 Materials

Octadecyl methacrylate (SMA, AR), methyl methacrylate (MMA, AR), butyl acrylate (BA, AR), dibenzoyl peroxide (BPO, AR), N,N'-methylenebis(2-propenamide) (MBA, AR), hexadecyl trimethyl ammonium bromide (CTAB, AR), ammonia water (AR), vinyltrimethoxysilane (VTMS), silica powder (SiO_2, AR), dichloromethane (AR), chloroform (AR), carbon tetrachloride (AR), dichloroethene (AR), toluene (AR), styrene (AR) and Tuwen 80 (AR) were purchased from Chengdu Kelon Reagent Co., Ltd. (Chengdu, China).

2.2 Preparation of modified SiO_2

A given weight of SiO_2 was fully dispersed in ethanol to prepare the suspension. Meanwhile, a given weight of VTMS was dissolved in ethanol and stirred at room temperature for 30 min to ensure complete dissolution. Then, the VTMS solution was slowly added to the SiO_2 suspension, and ammonia water (25-28 %) was used to adjust the mixture to pH=10. Finally, the mixture was stirred and reacted in a water bath for 4 h, and the system temperature was maintained at 40 ℃. The product was washed with deionized water five times and dried in a vacuum oven at 60 ℃ to obtain hydrophobic SiO_2 powder[19].

2.3 Preparation of PSA and PSA-SiO_2

First, a given weight of CTAB was dissolved in deionized water completely by utilizing a 250 mL three-neck flask with a stirrer, a reflux condenser, and a gas inlet pipe. The mixture of the monomers (SMA, MMA and BA), crosslinker (MBA) and initiator (BPO) were added to the CTAB aqueous solution in turn. Then, the polymerization was conducted under magnetic stirring at 75 ℃ for 5 h, followed by aging at 80 ℃ for 1 h. The product was washed with deionized water and ethanol three times and dried in a vacuum oven at 70 ℃ until it reached a constant weight to obtain P (SMA-*co*-MMA-*co*-BA) (PSA). Under the same synthesis conditions, SiO_2/P (SMA-*co*-MMA-*co*-BA) (PSA-SiO_2) could be prepared by adding modified SiO_2 with other monomers simultaneously. The final PSA and PSA-SiO_2 obtained are spherical particles (The figures of shape of PSA and PSA- SiO_2 are shown in Fig S1(a)).

2.4 Characterization

The structure of the composites was observed by infrared (IR) spectroscopy. FT-IR spectra were collected using KBr pellets of samples on a Nicolet IS 10 Fourier infrared spectrometer (wavenumber range of 4000~600 cm^{-1}). The surface

morphologies of the composites sprayed with gold pretreatment were observed by scanning electron microscopy (SEM) on SU8010. The water contact angle (WCA) of SiO_2 before and after modification was measured by a DSA20-Kruss type interface parameter integrated measurement system (measurement range was 0～180°, accuracy was ± 0.1°, and resolution was ± 0.01°). The specific surface area of the composites was measured by a Quadrasorb SI automatic specific surface area and porosity analyzer (the maximum degassing temperature was 300 ℃, the measurement range of the pore size was 0.5-50 nm, and the measurement range of the specific surface area was 0.01 m^2/g and above).

2.5 Performance Test

The yield of an oil-absorbing resin (P) was calculated by Equation (1).

$$P(\%)=\frac{m_R}{m_0}\times 100\% \quad (1)$$

Where, m_0 is the mass of obtained resin (g) and m_R is the mass of the initial raw materials used for the synthesis of the resin (g).

The oil absorbency (Q) testing approach was based on the gravimetric method[20], and Q was calculated by Equation (2).

$$Q(g/g)=\frac{m_T-m_0}{m_0} \quad (2)$$

where m_0 is the initial dry sample weight (g) and m_T is the weight of the sample at the end of the tests (g).

An ultraviolet–visible spectrophotometer (UV-1800) was used to measure the oil removal efficiency (η) of the O/W emulsion. According to the established concentration-absorbance standard curve, the initial oil concentration and the after-treatment oil concentration of the emulsion were calculated[21]. The oil removal efficiency (η) of the emulsion was calculated by Equation (3).

$$\eta\ (\%)=\frac{C_0-C_T}{C_0}\times 100\% \quad (3)$$

where C_0 is the initial oil concentration (mg/L) of the before-treatment emulsion and C_T is the oil concentration (mg/L) of the after-treatment emulsion.

All tests were performed in triplicate, and the results were the average of the three results from repeated tests.

3. Results and discussion

3.1 Optimization of polymerization system

3.1.1 Optimization of PSA

The synthesis conditions were optimized by orthogonal experiments, which were carried out by selecting the four-Factor L9 (3^4) orthogonal table. The orthogonal experimental scheme and results are shown in Table 1. It was indicated that the combination with the best adsorption capacity for $CHCl_3$ was $A_2B_2C_3D_1$. Preparing PSA with the best parameters, ω(MMA:BA) = 4:6, ω(SMA) = 3 %, ω(CTAB) = 0.3 %, and ω(MBA) = 0.7 %, could obtain the resin with the best oil absorbency for $CHCl_3$ in this polymerization system.

Table 1

Orthogonal experiment scheme and results of PSA

Factors influence and level	A ω(MMA:BA)	B ω(SMA)	C ω(CTAB)/%	D ω(MBA)/%
1	3:7	2	0.15	0.7
2	4:6	3	0.2	0.8
3	5:5	4	0.3	0.9

Experiment number		A	B	C	D	$CHCl_3$
1		1(3:7)	1(2)	1(0.15)	1(0.7)	27.91
2		1	2(3)	2(0.2)	2(0.8)	28.02
3		1	3(4)	3(0.3)	3(0.9)	26.27
4		2(4:6)	1	2	3	24.71
5		2	2	3	1	34.47
6		2	3	1	2	28.15
7		3(5:5)	1	3	2	21.87
8		3	2	1	3	20.36
9		3	3	2	1	22.16
$CHCl_3$	K_1	82.20	74.49	76.42	84.54	/
	K_2	87.33	82.85	74.89	78.04	
	K_3	64.39	76.58	82.61	71.34	
	k_1	27.40	24.83	25.47	28.18	
	k_2	29.11	27.62	24.93	26.01	
	k_3	21.46	25.53	27.54	23.78	
	R	7.65	2.79	2.61	4.40	

3.1.2 Optimization of PSA-SiO_2

Introducing the inorganic porous material SiO_2 into the polymerization system to improve oil-absorbing properties not only increased the pore structure and specific surface area but also supported the internal network structure when SiO_2 with an appropriate particle size and a certain amount was loaded with PSA.

Modified SiO_2 with varied particle sizes (10 to 500 nm) was introduced into the

polymerization system to delve into the influence of the particle size of SiO_2 on the performance of PSA-SiO_2. The oil absorbency of PSA-SiO_2 first increased and then decreased after reaching a peak as the particle size of SiO_2 increased, and the results are shown in Figure 1 (a). The reason could be that the aggregates were easily formed during polymerization, and the pores of the resin were blocked when the particle size was too tiny. Whereas the grafting chains of SiO_2 and acrylate monomers became shorter, resulting in difficulty forming an effective crosslinked network when the SiO_2 size was overly large[22].

When the particle size of SiO_2 was 10 nm, the BET specific surface area (S_{BET}) of the composite was 0.72 m^2/g. As the SiO_2 particle size increased to 50 nm, the S_{BET} increased to 1.67 m^2/g. However, when the SiO_2 particle size continued to increase to 500 nm, the S_{BET} decreased to 0.26 m^2/g, even lower than the PSA (0.44 m^2/g). This also confirmed the conclusion mentioned above.

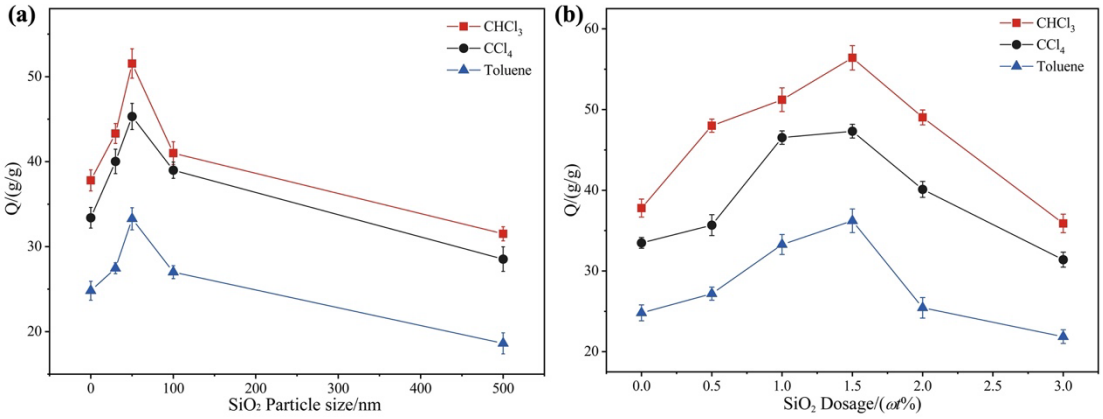

Figure 1 Effect of SiO_2 particle size (a) and dosage (b) on the absorbency of PSA-SiO_2

The effect of the dosage of SiO_2 on the oil absorbency of PSA-SiO_2 is shown in Figure 1 (b), where there was a trend of first increasing and then decreasing as the amount of modified SiO_2 was raised, with the largest oil absorbency for the 1.5 ωt% SiO_2 dose. If the amount of SiO_2 was small, the network structure was difficult to support, while the solvation was reduced because of the narrow internal network structure of the composite when the amount of SiO_2 was extreme, which affected the adsorption capacity[23]. The yields of PSA and PSA-SiO_2 prepared using the optimal system were 71.8 and 64.5 %, respectively.

3.2 Characterization

3.2.1 Characterization of FT-IR、Water contact angle and BET

Figure 2 (a) shows the FT-IR spectra of SiO_2 before and after hydrophobic modification. The absorption peak of curve (b) in Figure 2 (a) at 1633 cm^{-1} was attributed to the bending vibration of C=C[24]. Curve (b) in Figure 2 (a) exhibited three peaks at 2960, 2842 and 1409 cm^{-1}, corresponding to the Si-CH_3 symmetric stretching vibration, Si-CH_3 asymmetric stretching vibration and Si-CH_3 bending vibration, respectively[25]. The hydroxyl groups on the surface of SiO_2 were replaced by VTMS hydrolysates. The intensity and area of Si-O-Si stretching vibration, Si-O symmetric vibration and Si-O-Si bending vibration absorption peaks at 1085, 790, and 458 cm^{-1} of curve (b) in Figure 2 (a) were increased compared with curve (a) in Figure 2 (a). It was demonstrated that VTMS successfully modified SiO_2, and Si-O-Si bonds underwent accumulation, offering the possibility to break the emulsion of the composite after grafting the modified SiO_2[26,27].

Figure (b) and (c) shows the water contact angles (CA) of SiO_2 before and after hydrophobic modification. Due to the presence of hydroxyl groups on the surface of SiO_2, the water droplets in Figure 2 (b) spread rapidly across the surface of SiO_2, thus exhibiting hydrophilicity. However, the water droplets remained on the SiO_2 surface in Figure 2 (c), which was attributed to the -OCH_3 of VTMS becoming -OH after hydrolysis, and the vast majority of the -OH was dehydrated and condensed with the -OH on the SiO_2 surface, thereby introducing hydrophobic groups. The CA was altered from 9.7° to 139.1°, which proved that SiO_2 was successfully hydrophobically modified. Additionally, the figures of CA of PSA and PSA-SiO_2 were shown in the Fig S1(b).

Figure 2 (d) and (e) shows the adsorption-desorption isotherms of PSA and PSA-SiO_2 at -195.8 ℃ in a N_2 atmosphere. From the distribution diagram in Figure 2 (d), the adsorption-desorption isotherm of PSA belonged to the type IV isotherm. There

was an obvious adsorption hysteresis phenomenon at relative pressures of 0.6~1.0, indicating that there was a mesomultihole structure of PSA, which was conducive to the diffusion of oil molecules into the interior of the polymer[28]. Meanwhile, the adsorption-desorption isotherm of PSA-SiO_2 in Figure 2 (e) also belonged to the type IV isotherm. Its internal mesopores were smaller than those of PSA, which was mutually corroborated by the results for the pore size distribution in the pore diameter range of 2-9 nm. The specific surface areas of PSA and PSA-SiO_2 were 0.44 m^2/g and 1.67 m^2/g, respectively. The specific surface area of PSA-SiO_2 was larger, which was conducive to the diffusion of oil into the composite and thus improved the oil-adsorbing performance.

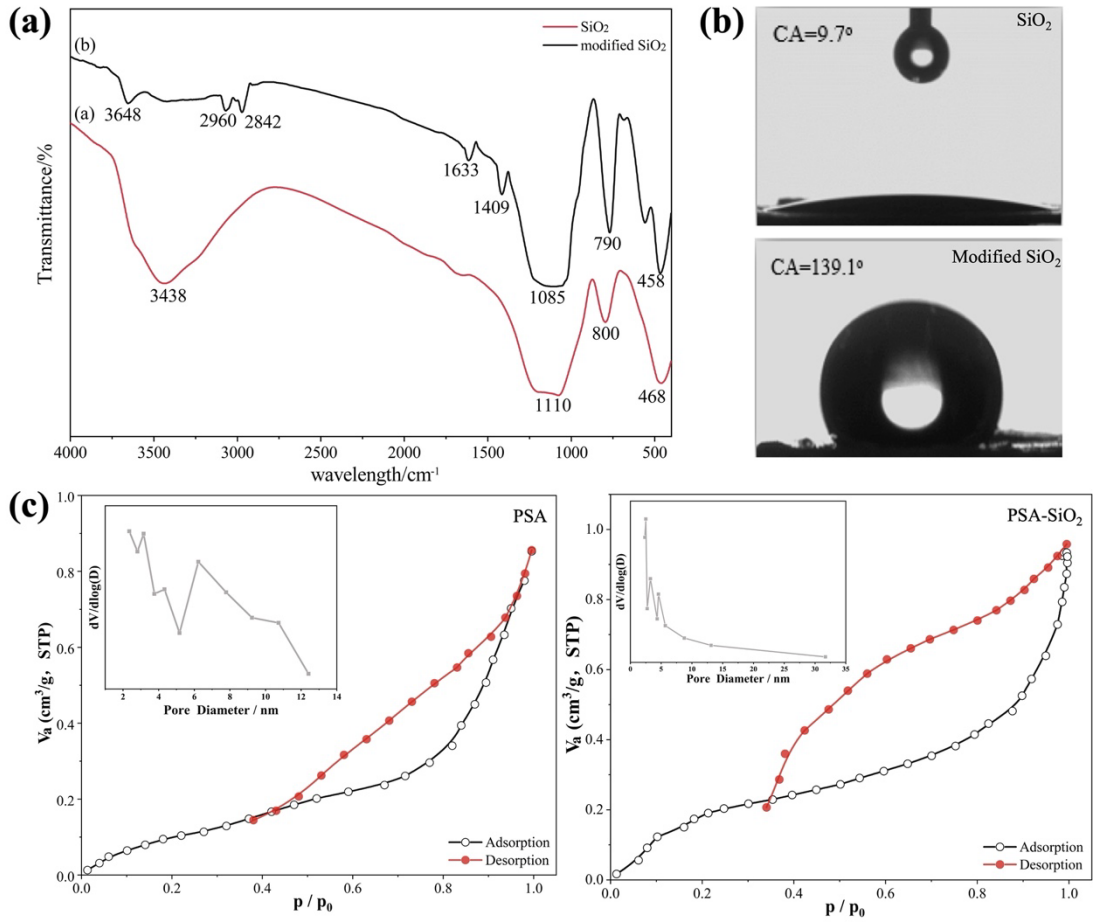

Figure 2 (a) FT-IR spectra of SiO_2 and modified SiO_2; (b) Water contact angle of SiO_2 and modified SiO_2; (c)Adsorption-desorption isotherm and pore diameter distribution diagram of PSA and PSA-SiO_2.

3.2.2 Characterization of SEM and EDS

Figure 3 shows the surface microstructure of PSA and PSA-SiO_2. Figure 3 (a) and (b) show the topography of PSA, which shows that the surface of the polymer was extremely smooth and presented tiny pores. Thus, the oil was arduous to enter the internal space. After introducing modified SiO_2, the surface of the composite in Figure 3 (c) became rough, and the multihole structure formed simultaneously. Then, numerous minor pores in Figure 3 (d) caused by mechanical agitation in the preparation process enriched the pore structure of the composite. The expanded contact area facilitated the oil-absorbing property improvement of PSA-SiO_2.

The EDS energy spectra of PSA and PSA-SiO_2 are shown in Figure 3 (e) and (f). The main elements of PSA and PSA-SiO_2 were C and O. However, PSA-SiO_2 contains Si; therefore, it was confirmed that hydrophobic SiO_2 was successfully introduced into the composite.

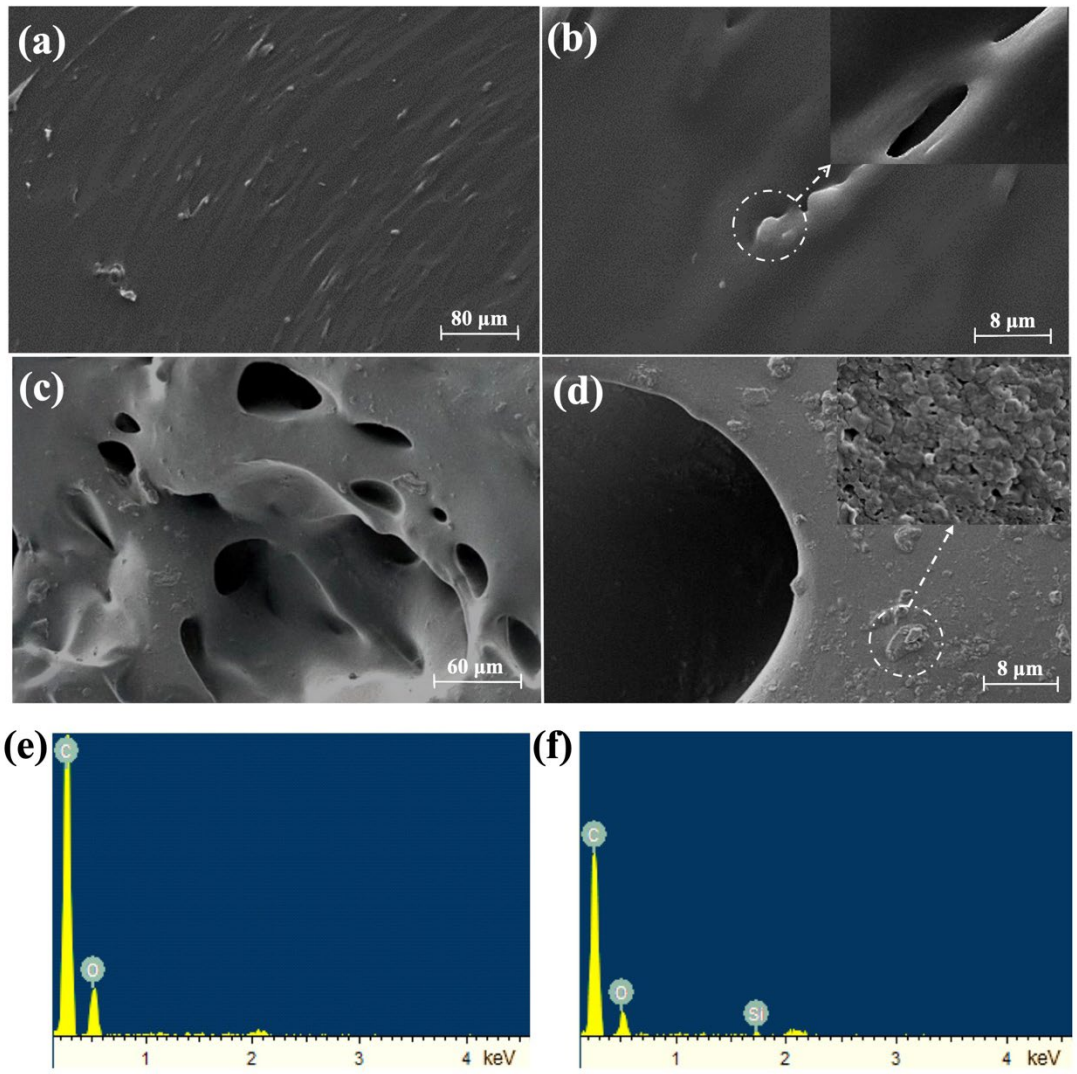

Figure 3 Microstructure of PSA (a), (b) and PSA-SiO_2 (c), (d); EDS energy appearance of PSA (e) and PSA-SiO_2 (f).

3.3 Oil-absorbing properties

Both PSA and PSA-SiO_2 displayed favorable adsorption capacity to common NAPLs, as shown in Figure 4, which compares the oil absorbency of the two materials on dichloromethane(CH_2Cl_2), chloroform($CHCl_3$), carbon tetrachloride(CCl_4), dichlorothene(C_2Cl_4), toluene and styrene.

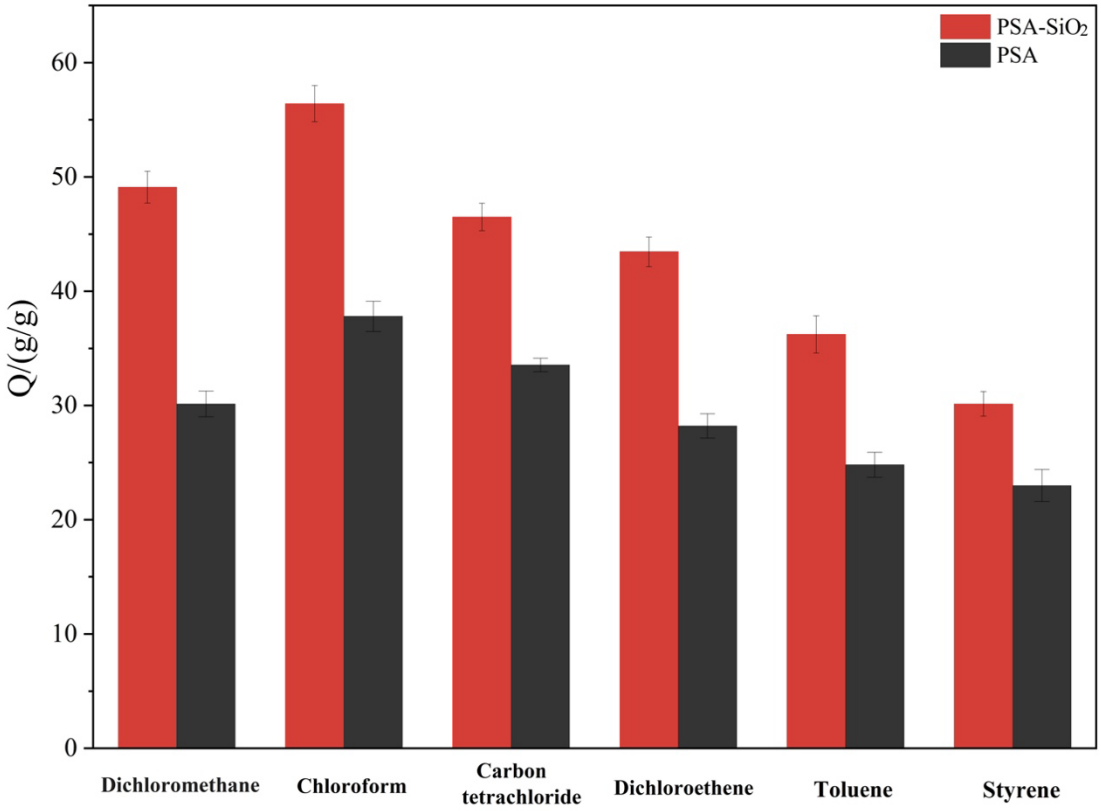

Figure 4 Oil Absorbencies of PSA and PSA-SiO_2

The oil absorbencies of PSA-SiO_2 for the above six NAPLs (49.10, 56.41, 47.32, 43.45, 36.22, and 30.14 g/g, respectively) were higher than those of unmodified PSA (30.14, 37.80, 33.55, 28.20, 24.81, and 23.00 g/g, respectively). Compared to PSA, PSA-SiO_2 showed a promotion of 62.91% in the oil absorbency of CH_2Cl_2, with the minimum enhancement in the oil absorbency being styrene, which increased by 31.04%. Apparently, the loading of modified SiO_2 could significantly improve the oil absorbency of the oil absorbent for partial NAPLs.

As frequently used chemical solvents, it has been a long struggled to eliminate the effects of toluene and $CHCl_3$ on the water environment. Therefore, the ability to adsorb both NAPLs is a crucial criterion to assess the properties of the oil absorbent.

Table 2 lists the comparison of the oil absorbencies of PSA-SiO_2 for toluene and $CHCl_3$ with other oil absorbents prepared in the literature.

Table 2

Comparison of oil absorbency from PSA-SiO_2 and other oil absorbents

Oil Adsorbent	Q/(g/g)		References
	Toluene	$CHCl_3$	
Cellulose/P(BMA-*co*-PETA)	15.40	29.00	[29]
CNFs/P(BA-*co*-BMA)	20.60	32.50	[30]
MnO_2/P(BA-*co*-BMA-*co*-MMA)	25.89	9.64	[31]
Poly(St-*co*-BMA-*co*-SAM)	12.34	23.00	[32]
Porous fibers/polyurethane foam	26.90	44.81	[33]
SiO_2/P(SMA-*co*-MMA-*co*-BA)	36.22	56.41	This Study

Clearly, for both toluene and $CHCl_3$, PSA-SiO_2 was superior to other oil-absorbing materials in terms of oil absorbency. Furthermore, these materials were only available for the treatment of pure oils and stratified oil-water mixtures, and no further research was done on the treatment of emulsion.

3.4 O/W emulsion treatment

3.4.1 Mechanism of one-step process of emulsion treatment

Due to its tunable surface properties and elevated interfacial activity, SiO_2 can be used in the construction of emulsion breakers. Si-O bonds have enhanced interactions with water and promote substitution reactions on surfactant interfacial films[34]. After the introduction of nano-SiO_2 modified by VTMS into the polymerization system, not only was the multihole structure of the composite enriched but also the special structure of the organosilicon ternary block was supplied, so that the composite may have demulsified performance.

The NAPLs were dispersed in water as tiny oil droplets after emulsification, and their oil-water boundary layer contained a certain amount of surfactant to form a stable O/W emulsion. The Si-O-Si bonds were the microstructure fragments of PSA-SiO_2. They could adsorb at the defect of the oil-water interface and destroy the structure of the surfactant aggregates even at extremely low concentrations, leading to final demulsification[35].

The one-step process of emulsion treatment is shown in Figure 5. The silicone triblock composite PSA-SiO_2 first adsorbed at the defect on the oil-water interface and then disrupted the surfactant aggregates, which in turn destroyed the oil-water

interface and caused the oil droplets to gather. Finally, PSA-SiO_2 adsorbed the aggregated oil and achieved oil remove form water of the emulsion in a one-step process.

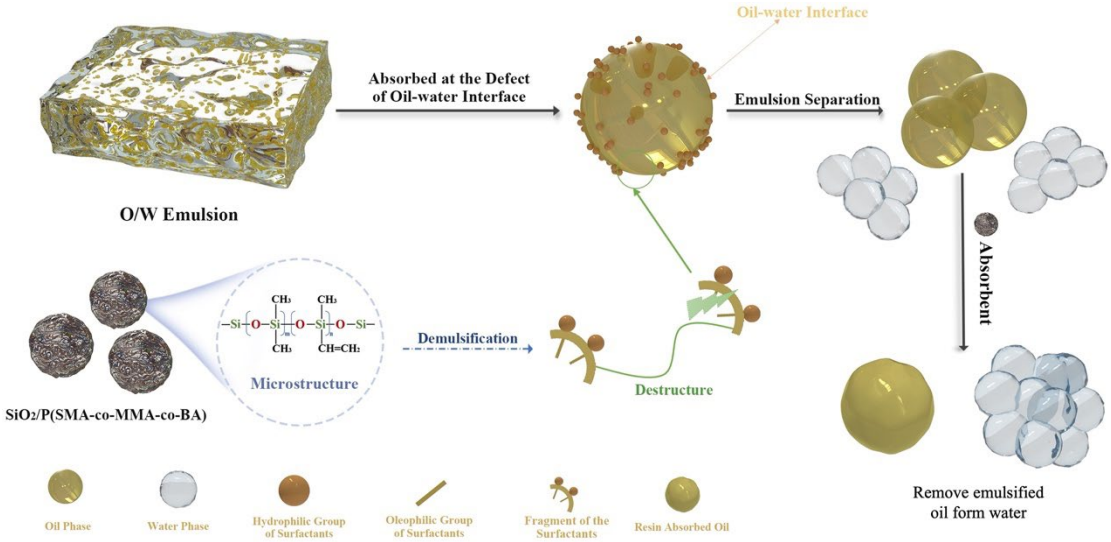

Figure 5 One-step process of emulsion treatment of PSA-SiO_2

3.4.2 Effect of the oil-water ratio of the emulsion

Figure 6 (a) shows the effect of the $CHCl_3$-water ratio on the oil removal efficiency of PSA-SiO_2. As the oil content in the emulsion decreased, the oil removal efficiency improved. When the oil-water volume ratio was 1:60, PSA-SiO_2 exhibited favorable oil removal efficiencies of 94.43% and 96.59% for the Tween 80-stabilized and CTAB-stabilized emulsions, respectively. When the oil content decreased continuously, the oil removal efficiency tended to plateau.

This phenomenon might be explained by the fact that the surfactant of the oil phase per unit volume decreased with the increment of the water phase in the emulsion. And then the oil-water interfacial tension decreased, leading to the coalescence of the oil droplets with each other, thus enlarging their size. However, emulsion retention and droplet stacking occurred after the excessively large-size oil phase entered the internal channels of PSA-SiO_2, forming a blocking layer that impeded oil adsorption after demulsification[36,37].

The $CHCl_3$-water emulsions were milky white before treatment and the oil droplets dispersed evenly in the water phase, as shown in Figure 6 (b). Then, the emulsion became clear and transparent after treatment, and almost all of the oil droplets were removed by PSA-SiO_2, with few oil droplets in water.

To further verify that demulsification occurred, the particle sizes of the oil phase before and after treatment are shown in Figure 6 (c) and (d). The particle sizes of

before-demulsified toluene and $CHCl_3$ were concentrated at 300-570 and 220-400 nm, respectively, while those of after-demulsified were concentrated at 4-19 and 3-5 nm, respectively. It was indicated that PSA-SiO_2 could be used to remove emulsified oil from water in the O/W emulsions in a one-step process.

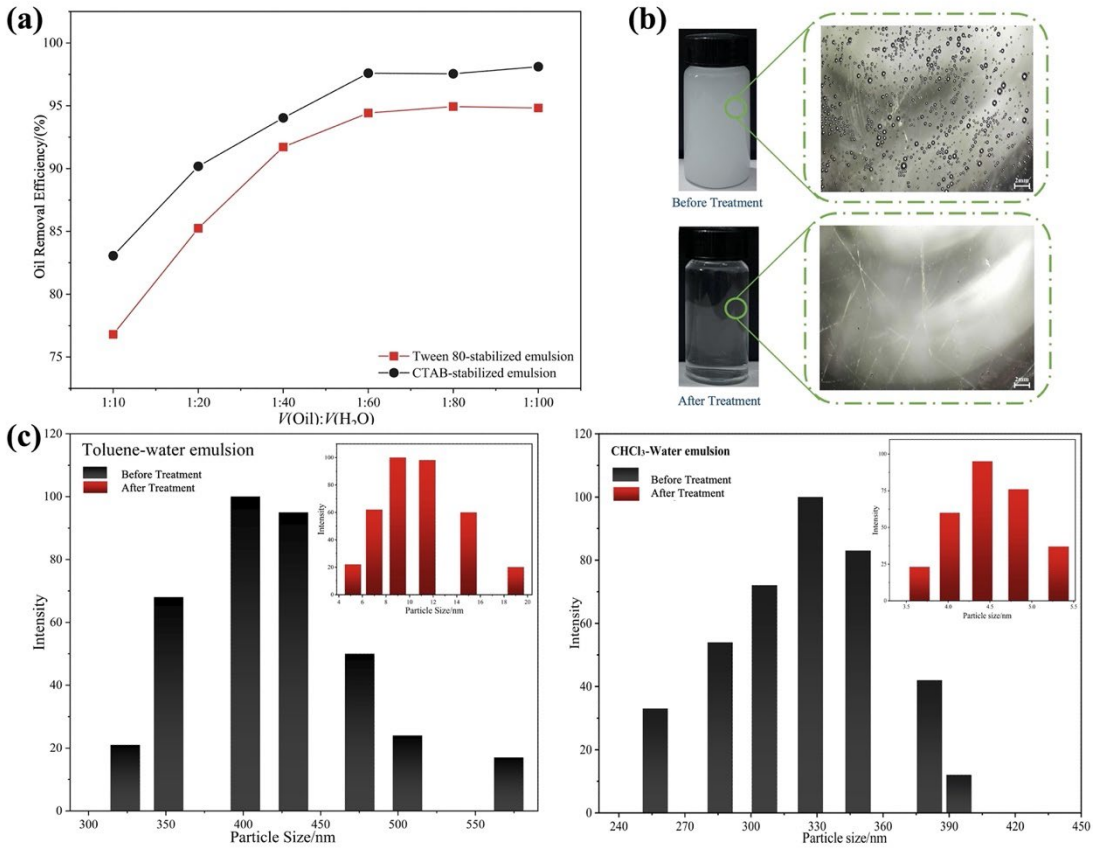

Figure 6 (a) Effect of the oil-water ratio on the oil removal efficiency; (b) $CHCl_3$-water emulsion (V($CHCl_3$):V(water)=1:60) before and after treatment; (c) Particle size of the oil phase in the emulsions before and after treatment under the condition of V(Oil):V(H_2O)= 1:60 in toluene-water and $CHCl_3$-water emulsion.

3.4.3 Rate of oil removal in the emulsion

The oil removal rates and efficiencies of PSA-SiO_2 for toluene-water and $CHCl_3$-water emulsions are shown in Figure 7. The oil removal efficiency of the Tween 80-stabilized, and CTAB-stabilized O/W emulsions increased rapidly within 2-7 h and reached equilibrium in the following 2 h. The final oil removal efficiency for the Tween 80-stabilized toluene-water and $CHCl_3$-water emulsions were 95.65% and 96.29%, respectively, and for the CTAB-stabilized toluene-water and $CHCl_3$-water emulsions were 94.88% and 98.11%, respectively. PSA-SiO_2 had a favorable demulsification and adsorption capacity for toluene-water and $CHCl_3$-water

emulsions.

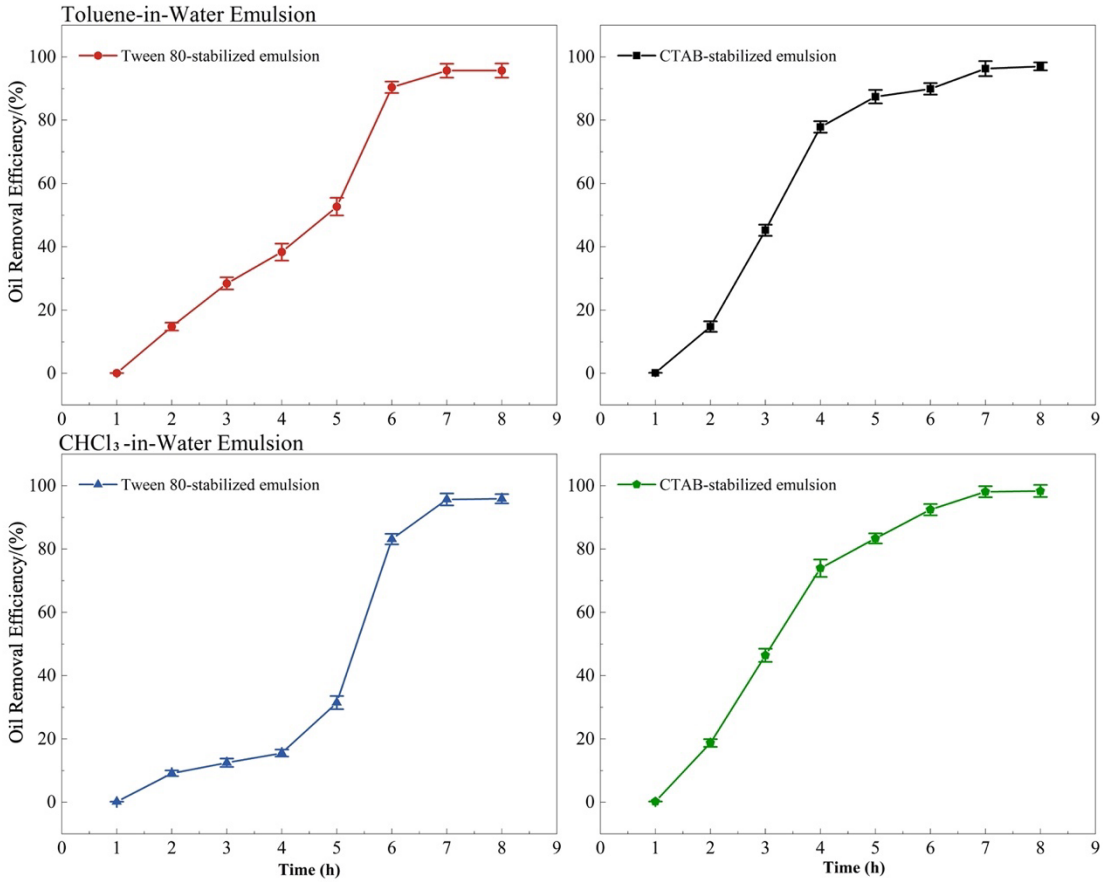

Figure 7 Oil removal efficiency of PSA-SiO_2 for Tween 80-stabilized and CTAB-stabilized emulsions under the condition of V(Oil):V(H_2O)= 1:60

3.4.4 Properties of continuous oil removal and reusability of PSA-SiO_2

When the dosage of PSA-SiO_2 was 5 g/L, the composite was taken out after the end of the oil removal form emulsion and placed in another emulsion to continue to remove oil in the next experiment, after which the composite was desorbed by ethanol at the last time experiment. Then, a same experiment repeated with this desorbed composite. The continuous oil removal efficiencies and reusability capabilities of PSA-SiO_2 are shown in Figure 8.

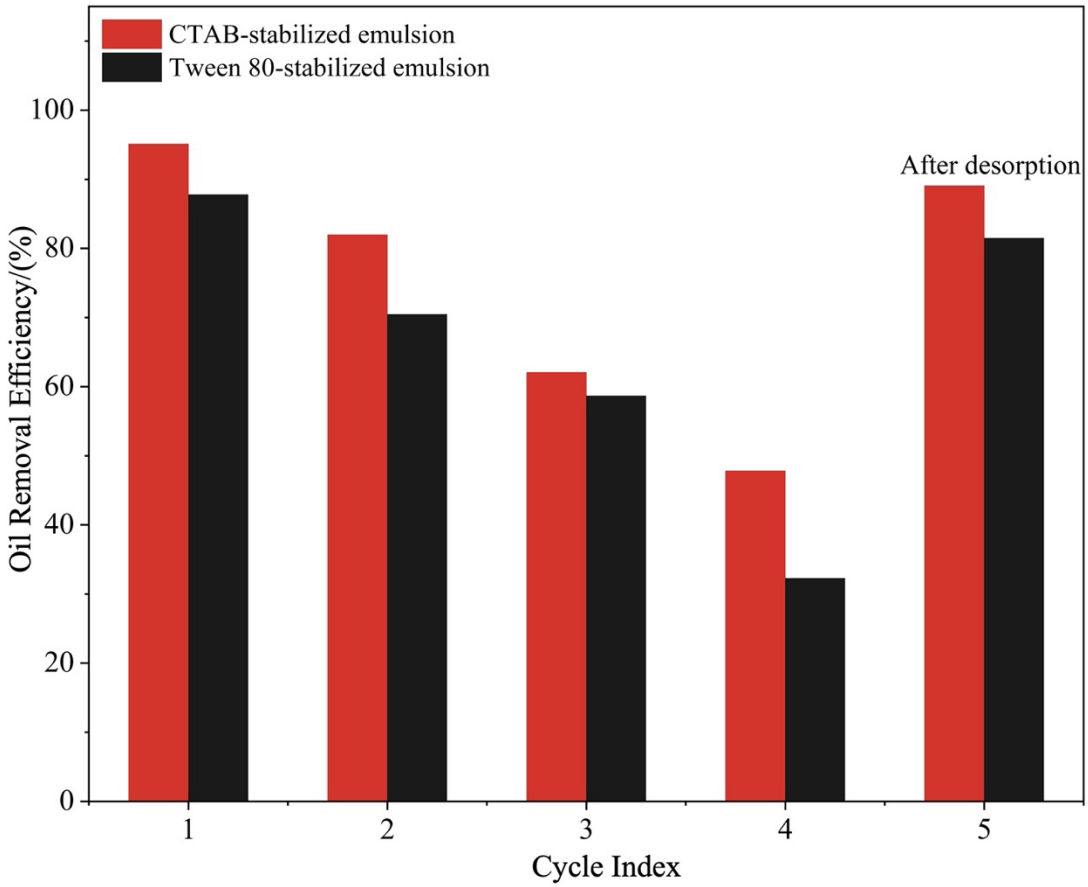

Figure 8 Oil removal efficiencies and reusability capabilities of PSA-SiO_2 for Tween 80-stabilized and CTAB-stabilized emulsions under the conditions of V(Oil):V(H_2O)= 1:60 and treatment time=7 h

Since the saturated absorbency of PSA-SiO_2 was not reached by emulsion treatment of single time, iterative oil removal in the O/W emulsion could be performed. As the number of continuous oil removal increased, the oil removal efficiency of the emulsions gradually decreased. In the fourth run, the oil removal efficiency decreases to 32.31% and 47.83% for Twain 80-stabilized and CTAB-stabilized emulsions, respectively. Nonetheless, the oil removal capacity of PSA-SiO_2 could be recovered after desorption by ethanol. PSA-SiO_2 had promising properties of continuous oil removal and reusability of emulsion treatment for Tween 80-stabilized and CTAB-stabilized $CHCl_3$-water emulsions.

4. Conclusion

An organic–inorganic composite PSA-SiO_2 was successfully synthesized by loading nanoparticle SiO_2 as a functional material into polyacrylate. The results of FT-IR, SEM–EDS and BET indicated that SiO_2 was hydrophobically modified and

successfully introduced into the acrylate polymerization system. It was demonstrated that the introduction of SiO_2 could effectively enrich the multihole structure of polymers and add functionality to organosilicon triblock copolymers. PSA-SiO_2 exhibited favorable oil absorbency for some common pure NAPLs (49.10, 56.41, 47.32, 43.45, and 36.22 g/g for $CHCl_3$, CCl_4, C_2Cl_4, toluene and styrene, respectively). In addition, PSA- SiO_2 exhibited satisfactory demulsification and oil removal capacities on O/W emulsions, achieving oil removal efficiencies of 95.65%, 96.29%, 94.88% and 98.11% for Tween 80-stabilized and CTAB-stabilized toluene-water and $CHCl_3$-water emulsions, respectively. As a result, the PSA-SiO_2 composite not only had strong oil absorbencies on common pure NAPLs but also incorporated oil adsorption and demulsification capacities for emulsion, enabling to remove emulsified oil droplets from water in a one-step process. This study provides a promising strategy for potential applications in oily wastewater treatment.

Author Contributions

Y. J. Zhou put forward a concept, designed the experiments, and wrote the original draft. Y. J. Zhou, F. Li, Y. Q. Liu, and H.Y. Qiu grew the detailed experimental methodology and data analysis. G. H. Lan designed and supervised the experiments. X. Bo and K.Y. Pu reviewed and editing the manuscript. W.R. Dai and X.Y. Zhang performed the experiments. All the authors discussed the results and commented on the manuscript.

Conflicts of interest

The authors declare no competing financial interests.

Supplementary Information

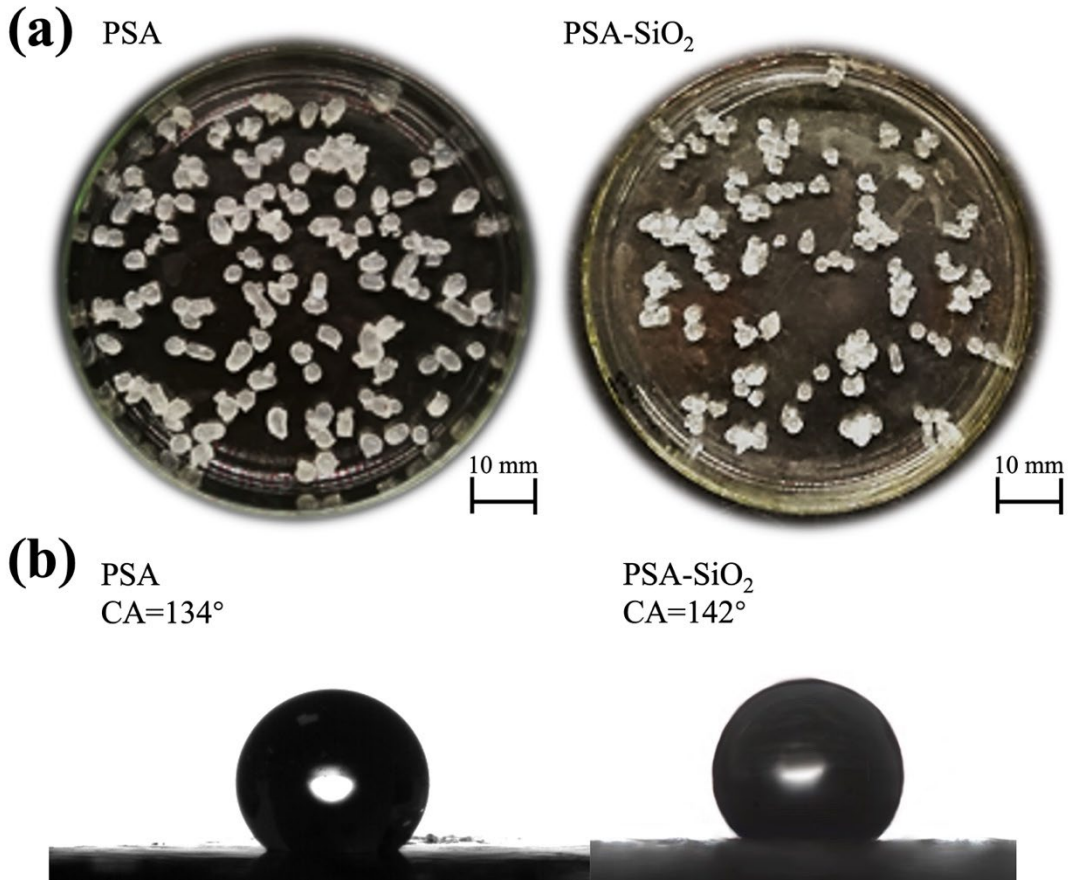

Figure S1 (a) Shape of PSA and PSA-SiO_2 ; (b) Contact angle of PSA and PSA-SiO_2.

Due to the aggregation process, the PSA and PSA-SiO_2 prepared are in the form of spherical particles. To conduct contact angle testing, we did not add any stabilizer to the polymerization system, resulting in the prepared composites being in block form. Therefore, there were a certain degree of error in the contact angle data.

References

[1] Ren, J.G., et al., Research progress on remediation technology of chlorinated hydrocarbon pollution in groundwater[J]. Environmental scientific research, 2021, 34(7): 1641-1653. https://doi.org/10.13198/j.issn.1001-6929.2021.01.07

[2] Iva, Dolinová, Marie, et al. Dynamics of organohalide-respiring bacteria and their genes following in-situ chemical oxidation of chlorinated ethenes and biostimulation[J]. Chemosphere, 2016. https://doi.org/10.1016/j.chemosphere.2016.05.030

[3] Ewaid, S.H., et al., Acute toxicity of the water chlorination byproduct (chloroform) in male mice[C]. AIP Conference Proceedings, 2020(1): 1-6.

[4]Yuan, H., et al., Demulsification of Water-Containing Crude Oil Driven by

Environmentally Friendly SiO_2@CS Composite Materials[J]. Energy & Fuels, 2020, 34(7): 8316-8324. https://doi.org/10.1021/acs.energyfuels.0c01660

[5] Zhao, B., et al., Eco-friendly separation layers based on waste peanut shell for gravity-driven water-in-oil emulsion separation[J]. Journal of Cleaner Production, 2020, 255: 120184. https://doi.org/10.1016/j.jclepro.2020.120184

[6] Liu, C., et al., Precontrol of algae-induced black blooms through sediment dredging at appropriate depth in a typical eutrophic shallow lake[J]. Ecological Engineering, 2015, 77: 139-145. https://doi.org/10.1016/j.ecoleng.2015.01.030

[7] Zhang, T., et al., Hybridization of Al_2O_3 microspheres and acrylic ester resins as a synergistic absorbent for selective oil and organic solvent absorption[J]. Applied Organometallic Chemistry, 2018, 32(4): (e4244). https://doi.org/10.1002/aoc.4244

[8] Yan L., Li Q., and Wang X., et al., Synthesis and Absorption Performance of Acrylic Ester and Hollow Fiber MgO Nanoparticle Resin Composite[J]. Polymer-Plastics Technology and Engineering, 2017: 1-9. https://doi.org/10.1080/03602559.2017.1295310

[9] Liu H., Wang H., and Jia W., et al., Preparation and properties of magnetic–photoresponsive oil-absorption resins[J]. Journal of Applied Polymer Science, 2017: 45756. https://doi.org/10.1002/app.45756

[10] Li, J., et al., Preparation and application of supported demulsifier PPA@SiO_2 for oil removal of oil-in-water emulsion[J]. Separation science and technology, 2020, 55(14): 2538-2549. https://doi.org/10.1080/01496395.2019.1634733

[11] Na A, et al. Interfacially active and magnetically responsive composite nanoparticles with raspberry like structure; synthesis and its applications for heavy crude oil/water separation[J]. Colloids and Surfaces A: Physicochemical and Engineering Aspects, 2015, 472:38-49. https://doi.org/10.1016/j.colsurfa.2015.01.087

[12] Mu, Y., et al., Preparation and demulsification performance of modified attapulgite nanoparticle demulsifier[J]. Fuel, 2022, 313: 123038. https://doi.org/10.1016/j.fuel.2021.123038

[13] Xu, H.Y., Jia, W.H., and Ren, S.L., et al. Magnetically responsive multi-wall carbon nanotubes as recyclable demulsifier for oil removal from crude oil-in-water emulsion with different pH levels - ScienceDirect[J]. Carbon, 2019, 145: 229-239. https://doi.org/10.1016/j.carbon.2019.01.024

[14] Ren, S.L., et al. Separation of Emulsified Oil from Oily Wastewater by Functionalized Multiwalled Carbon Nanotubes[J]. Journal of Dispersion Science &

Technology, 2016.
[15] Mei, H. Z., Ha, C., Cho, W. Synthesis and properties of high oil-absorptive network polymer 4-tert-butylstyrene–SBR–divinylbenzene[J]. Journal of Applied Polymer Science, 2010, 81(5). https://doi.org/10.1002/app.1550
[16] Atul Kumar Maurya., Rajesh Mahadeva., Gaurav Manik., Shashikant P. Patole. An investigation into performance properties of sustainable polypropylene composites reinforced with basalt fiber and fly ash[J]. Polymer Composites, 2023, 44(8): 5104-5120. https://doi.org/10.1002/pc.27476
[17] Singh M., Sethi S K., Manik G. Pressure-sensitive adhesives based on acrylated epoxidized linseed oil: A computational approach[J]. 2021. https://doi.org/10.1016/j.ijadhadh.2021.103031
[18] Singh M., Manik G. Computationally developed acrylated epoxidized methyl ester based pressure-sensitive adhesives[J]. 2023, 228. https://doi.org/10.1016/j.commatsci.2023.112329
[19] Yang, H., and Chen, F., Study on the superhydrophobic modification of silica by vinyl trimethoxysilane[J]. Journal of intraocular lens, 2015, 44(09): 2597-2605. https://doi.org/ 10.16553/j.cnki.issn1000-985x.2015.09.051
[20] Wang, X.H., Synthesis of Acrylic High-Oil Absorption Resins[J]. Advanced Materials Research, 2012. 502: 222-226. https://doi.org/10.4028/www.scientific.net/AMR.502.222
[21] Kang, H.X., Sup, S., U.S. Sup and L.S. Sup, Preparation of underwater superhydrophobic film and separation performance of oil-in-water emulsion[D]. Journal of Lanzhou Jiaotong University, 2019(5): 96-104.
[22] Pinho L., Mosquera M J., Photocatalytic activity of TiO_2–SiO_2 nanocomposites applied to buildings: Influence of particle size and loading[J]. Applied Catalysis B Environmental, 2013, 134(Complete): 205-221. https://doi.org/10.1016/j.apcatb.2013.01.021
[23] Song C., Ding L., Yao F., et al. β-Cyclodextrin-based oil-absorbent microspheres: Preparation and high oil absorbency[J]. Carbohydrate Polymers, 2013, 91(1): 217-223. https://doi.org/10.1016/j.carbpol.2012.08.036
[24] Kong, L., et al., Synthesis of a novel oil-absorption resin and optimization of its performance parameters using response surface design[J]. Polymers for Advanced Technologies, 2019, 30(6): 1441-1452. https://doi.org/10.1002/pat.4576
[25] Chen, Y.Z., Ou, Z.W., Liu, Z.H., et al., Preparation technology and application of

silica aerogel[J]. Contemporary Chemical Industry, 2017, 46(10): 5.
[25] Bazmandegan-Shamili., et al., MultiSimplex optimization of the dispersive solid-phase microextraction and determination of fenitrothion by magnetic molecularly imprinted polymer and high-performance liquid chromatography[J]. Journal of the Iranian Chemical Society, 2018, 15(5). https://doi.org/ 10.1007/s13738-018-1316-0
[27] Zhang, W., et al., Superhydrophobic and Superoleophilic PVDF Membranes for Effective Separation of Water-in-Oil Emulsions with High Flux[J]. Advanced Materials, 2013. 25(14): 2071-2076. https://doi.org/10.1002/adma.201204520
[28] Chen, J.Z., Xu, J.L., et al., Nitrogen-doped hierarchically porous carbon foam: a free-standing electrode and mechanical support for high-performance supercapacitors[J]. Nano Energy, 2016: 193-202. https://doi.org/10.1016/j.nanoen.2016.04.037
[29] Fan, L., Chen, H., Hao, Z., et al. Cellulose-based macroinitiator for crosslinked poly (butyl methacrylate-*co*-pentaerythritol triacrylate) oil-absorbing materials by SET-LRP[J]. Journal of Polymer Science, Part A: Polymer Chemistry, 2013, 51(2): 457-462. https://doi.org/10.1002/pola.26404
[30]Chen G.Y., Cao, Y.R., Ke, L., et al. Plant polyphenols as multifunctional platforms to fabricate three-dimensional superhydrophobic foams for oil/water and emulsion separation[J]. Industrial and Engineering Chemistry Research, 2018, 57(48): 16442-16450. https://doi.org/10.1021/acs.iecr.8b03953
[31] Zhang, C., Yang, D.Y., Zhang, T., et al. Synthesis of MnO_2/poly(n-butylacrylate-*co*- butyl methacrylate-*co*-methyl methacrylate) hybrid resins for efficient oils and organic solvents absorption[J]. Journal of Cleaner Production, 2017, 148: 398-406. https://doi.org/10.1016/j.jclepro.2017.02.009
[32] Fang, P., Mao, P.P., Chen, J., et al. Synthesis and properties of a ternary polyacrylate copolymer resin for the absorption of oil spills[J]. Applied Polymer, 2014, 131(8): 40180. https://doi.org/10.1002/app.40180
[33] Zhang ,T., Kong, L.Y., Zhang, M.Y., et al. Synthesis and characterization of porous fibers/polyurethane foam composites for selective removal of oils and organic solvents from water[J]. RSC Advances, 2016, 6(89): 86510-86519. https://doi.org/10.1016/j.compositesa.2010.11.004
[34] Wang, T., et al. Fuzzy Reliability Design of Robot Parts Based on Weibull and Normal Distribution[C]. International Conference on Computer Science and Software Engineering. 2008: 1081-1084. https://doi.org/10.1109/CSSE.2008.430

[35] Zhou, J.J., et al., Nano-modification of carboxylated polyether for enhanced room temperature demulsification of oil-water emulsions: Synthesis, performance and mechanisms[J]. Journal of Hazardous Materials, 2022: 129654.
https://doi.org/10.1016/j.jhazmat.2022.129654
[36] Wang, X., Synthesis and characterization of polyolefin grafted polybutadiene copolymer[D]. Dalian, China: Dalian University of Technology, 2014.
[37] Zhang, F.F., Effect of SiO_2 morphology and particle size on dielectric properties of polyolefin composite resin[D]. Chengdu, China: University of Electronic Science and Technology of China, 2019.